VOL. 18, NO. 18, SEPTEMBER 2023 ISSN 1819-6608
ARPN Journal of Engineering and Applied Sciences

www.arpnjournals.com

FLUID DYNAMIC DESIGN OF A VERTICAL AXIS WIND TURBINE ROTOR UNDER LOW WIND SPEED

Jesús D. Rhenals-Julio, Omar D. Perez, Luis G. Vidal, Arnold Martínez Guarín and Jorge M. Mendoza
Department of Mechanical Engineering, University of Córdoba, Carrera Montería, Colombia
E-Mail: jesusrhenalsj@correo.unicordoba.edu.co

ABSTRACT

The design of the rotor geometry of a vertical axis wind turbine (VAWT) type H, for power generation at low wind speeds, is presented. The computational simulation allowed us to establish that the NACA 0018 profile offers a better ratio of lift and drag coefficients in contrast to NACA 0021 and NACA 0025, so this geometry was selected as the working profile. Then, to generate a power of 30W, the dimensions of the airfoil chord, the radius, and the rotor's height were found from the blade tip speed ratio (TSR) values and the power coefficient. The results obtained indicate that the appropriate dimensions of the rotor at low-speed conditions are, a diameter of 2 m, a height of 2.16 m, and several blades of 3, for a rotation speed of 9 rad/s. Finally, an agreement was found between the angular velocity calculated theoretically, for the proposed rotor dimensions, and that obtained from the ANSYS-CFD simulation.

Keywords: wind turbine, VAWT, CFD, airfoil.

Manuscript Received 6 April 2023; Revised 11 November 2023; Published 30 November 2023

1. INTRODUCTION

The world is undergoing a transition in terms of energy generation sources, focusing on cleaner forms of energy to reduce the high dependence on fossil fuels [1]. Wind energy is one of the alternatives that has taken more strength in recent decades, of there are different variations in terms of geometry and shape, among these are the horizontal axis wind turbines (HAWT) and vertical axis wind turbines (VAWT), the first being the most complex application because they require high wind speeds, large structures and high efficiency to recover sufficient wind flow and take advantage of the force of wind movement [2], while vertical axis wind turbines are suitable for remote or urban environments with low speeds, since they can be designed at more acceptable scales and installed on roofs or buildings, without limitations in noise level and at low cost [3].

In the literature there are several studies on the analysis of optimal airfoils for power generation at low speeds, being the CFD method one of the most used tools for this purpose. However, it is still a challenge to accurately simulate the transition between the laminar and turbulent layer on the blade surface [4], which makes it necessary to select a good turbulence model to ensure that the results are as accurate as possible. For Reynolds higher than 1x106 satisfactory studies have been carried out with the Transition SST model [5], and likewise, with the k-e turbulence model, at Reynolds values close to $1x10^5$ [6].

Regarding VAWT design, Darrieus H-type or giromill rotors are widely used for power generation purposes at low Reynolds numbers [7]. The literature presents some studies on the design of vertical axis wind turbines, Almanza & Rodriguez [8], designed a turbine capable of producing 1 kW of energy with a wind speed of 5.98 m/s, using analytical techniques to estimate the dimensions of the rotor, finally concluded that although wind energy is a clean form of energy, the manufacture of low power turbines can present a severe environmental impact. For their part Murshed *et al.* [9] performed the analysis of an aerodynamic profile and designed the blades of a turbine up to 10 meters high, for the coastal areas of Bangladesh, for this, they selected the optimum profile using the panel method, finding in their final design that the turbine was capable of generating up to 250 W at a wind speed of 3.437 m/s.

Similarly, Gonzalez-Diaz *et al.* [10] performed a wing geometry design to operate with the wind speeds of the province of Cordoba in Colombia, the calculated rotor had dimensions of; 2 m in height, a chord length of the profile of 0.55 m, and a rotor diameter of 2.6 m obtaining with this an increase of the nominal captured power of 17.19 W up to 45.57 W and a maximum power of approximately 400 W, finally recommending to select other turbulence models different from the k-w due to the atypical behavior of the Cp.

Lanzafame *et al.* [11], developed a 3D CFD model to predict the performance of wind turbines and evaluate the capabilities of the 1D models proposed according to the BEM theory (Blade element momentum theory) using the k-w SST and k-w turbulence models. By comparing the obtained results with the experimental data, they conclude that for this type of turbines the k-w model predicts better results than the k-w SST model.

Balduzzi *et al.* [12] performed an in-depth analysis to determine the considerations in the CFD models that allow to effectively predict the behavior of a Darrieus H-type vertical axis turbine. Additionally, they evaluated the necessary adjustments to avoid instability in the flows over this type of turbines, finally they concluded that k-ω SST turbulence model more realistically models the behavior of Darrieus turbines, since it takes into account the effects of boundary layer separation and free

VOL. 18, NO. 18, SEPTEMBER 2023 ISSN 1819-6608
ARPN Journal of Engineering and Applied Sciences

www.arpnjournals.com

shear flows. Furthermore, they found that the solution scheme based on pressure coupled compressible flow is the best numerical approach for the solution of this type of problems.

The purpose of this work is to design the H-type darreius rotor of a vertical axis wind turbine, capable of generating power in cities with low wind speeds, as an alternative and contribution to the search for new and more efficient renewable energy sources. Due to the limitations of the k-w turbulence model reported in the literature, for this work, the k-w SST turbulence model will be used, which combines the basic k-e model with the k-w model, which has been successfully applied in a low Reynolds number analysis [13], [14].

2. MATERIALS AND METHODS

The methodology implemented in this work consists of five stages to obtain the optimal rotor geometry, which are described below.

2.1 Airfoil Preselection

Based on the studies found and their efficiency in the use of H-type wind turbines, the pre-selected symmetrical airfoils were; NACA 0018, for its high lift-drag coefficient ratio at lower angles of attack [8], followed by NACA 0021 for its commercial availability, wide operating range and maximum performance with optimum efficiency [9], and finally, NACA 0025, for working with good lift loads at high angles of attack, maintaining a low drag coefficient and a good lift-drag ratio [10].

2.2 Evaluation of Drag and Lift Coefficients in CFD

At this stage, the CFD method is used to evaluate the values of the coefficients in each preselected profile. This is done with the help of ANSYS-FLUENT 22.1 software, based on the pressure-based solution method and a k-w SST turbulence model.

Subsequently, with data obtained from literature, the dimensions of the computational fluid domain were set as follows; 25 times the chord in upper, lower and left lateral directions to the profile, while, in the right direction of 50 times the chord, for the flow development. These dimensions have proven to be favorable in the study of airfoils [15].

As for the meshing, it was carried out with a dimension of 0.5 m per element, but it was necessary to divide the blade edge into 300 parts for greater precision in the variables studied on it. For the same purpose, the inflation command is inserted around the wing surface, with 100 divisions that increase at a rate of 1.2 to the previous one, thus considering more details in the viscous and pressure effects generated by the fluid-surface interaction. Figure-1 shows the dry grid of the airfoil and away from the airfoil.

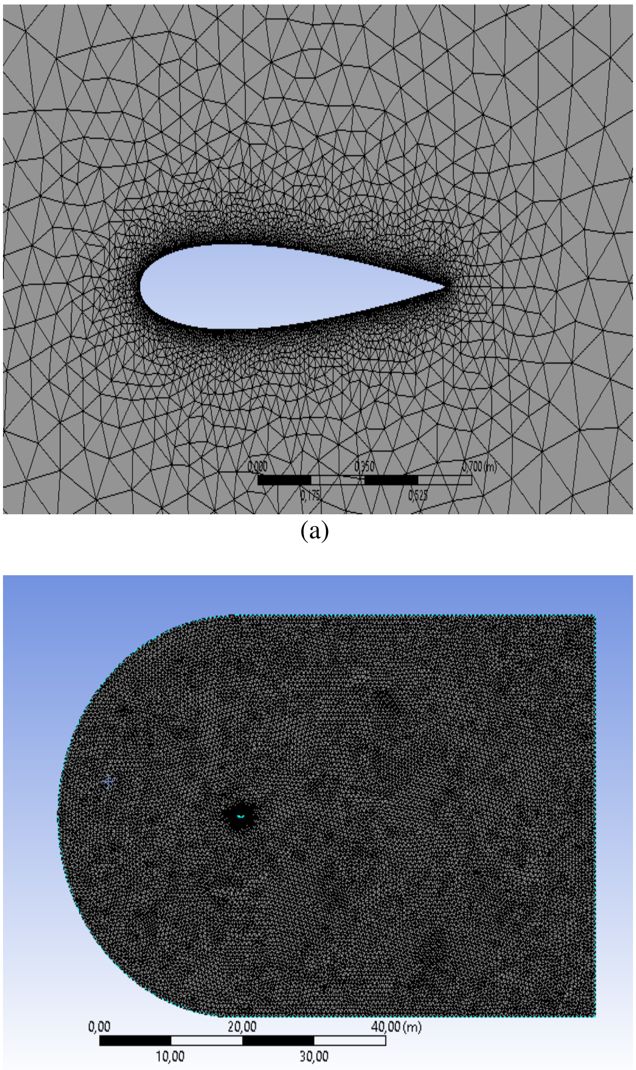

(b)

Figure-1. Meshing of the computational domain (a) near the airfoil and (b) in the full computational domain.

Initially, for the flow outlet and at the domain walls, we worked under ambient conditions, i.e., gauge pressure of 0 Pa and temperature of 300 K, giving the boundary conditions (including the profile) characteristics of smooth non-slip walls for no unwanted flow disturbance [16].

In obtaining the results, the values of the drag and lift forces were generated, which are the forces in the x-axis and y-axis, respectively. With the above, the drag and lift coefficients of each of the pre-selected profiles are determined.

The lift coefficient (C_L) is a dimensionless quantity that depends on the lift force (L) on the airfoil due to the distribution of pressures on the airfoil and the distribution of shear stresses. As defined in equation (1).

$$C_L = \frac{L}{0{,}5 \cdot \rho \cdot V^2 \cdot S} \quad (1)$$

VOL. 18, NO. 18, SEPTEMBER 2023 ISSN 1819-6608
ARPN Journal of Engineering and Applied Sciences

www.arpnjournals.com

On the other hand, the drag coefficient (C_D) is a dimensionless quantity that depends on the drag force (D) and was calculated as shown in equation (2).

$$C_D = \frac{D}{0{,}5 \cdot \rho \cdot V^2 \cdot S} \tag{2}$$

Where ρ is the fluid density; V is the fluid velocity and S is the wing area, which by convention is considered equal to the value of the wing chord.

2.3 Airfoil Selection

Once the values obtained in the two previous stages have been compared and validated, the airfoil with the highest drag-sustenance ratio and with a slight variation of the lift coefficient concerning the angle of attack is selected.

2.4 Rotor Design

The values of blade tip speed (TSR), power coefficient (Cp), and rotor robustness (σ) are established and tabulated. From the above, by setting a given number of blades and a desired rotor radius, the optimum chord length, rotor height and required angular velocity are found.

2.5 CFD Validation of the Rotor

A transient state study was performed, under the same SST k-w turbulence model. The domain used was a rectangular area whose dimensions depended on the rotor diameter, and likewise, a circular area of 1.25 times the rotor diameter was specified, as shown in Figure-2.

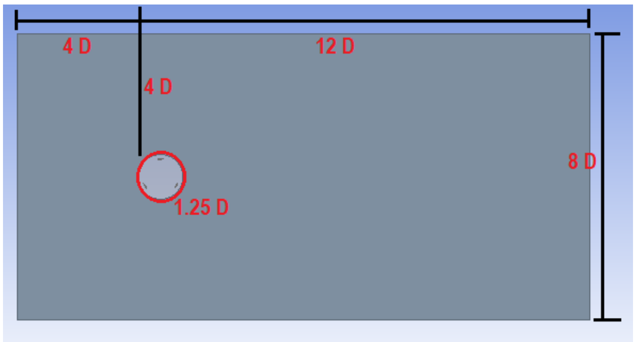

Figure-2. Computational domain.

For the meshing, the inflation command was used for the blade edges, working with an element size of 0.05 m for the inner domain and 0.1 m for the outer domain. Figure-3 shows the meshing of the computational domain defined for the wind turbine.

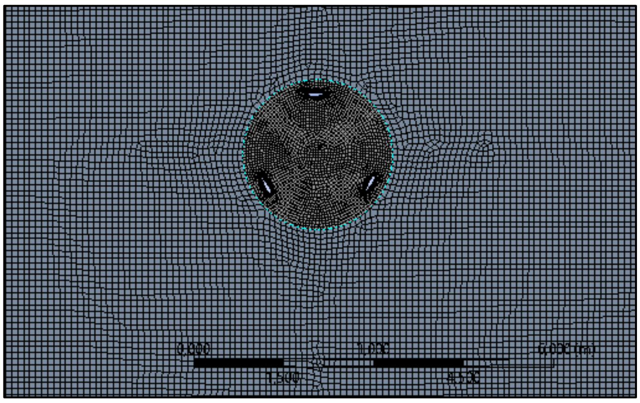

Figure-3. Meshing of the computational domain for the wind turbine.

During processing, a dynamic mesh was specified for the rotor zone, allowing for blade interaction with wind speeds, and an area-weighted average report was created for the tangential velocity experienced by the blades. 300-time steps were chosen, with intervals of 0.005 seconds between each other, giving us a simulation of 1.5 seconds. A maximum number of 10 iterations were defined for each step.

3. RESULTS AND DISCUSSIONS

3.1 Drag and Lift Coefficients of the Airfoils

Figure-4 shows the coefficients and the polar curve of each of the airfoils at different angles of attack. For airfoil NACA 0018 it is found that at 15° it has a higher lift coefficient than the rest, however, between the angles of 8° to 12° it has lower values. The behavior of the coefficient curves for the NACA 0021 profile is intermediate between the values of the rest of the profiles, although at approximately 9° it has slightly higher values. The latter, together with NACA 0021 have an unfavorable behavior in their lift coefficient, just in the zone where they are superior to the NACA 0018 profile, since they reach a maximum value and then tend to decrease, although later they again have increasing values.

VOL. 18, NO. 18, SEPTEMBER 2023 ISSN 1819-6608
ARPN Journal of Engineering and Applied Sciences

www.arpnjournals.com

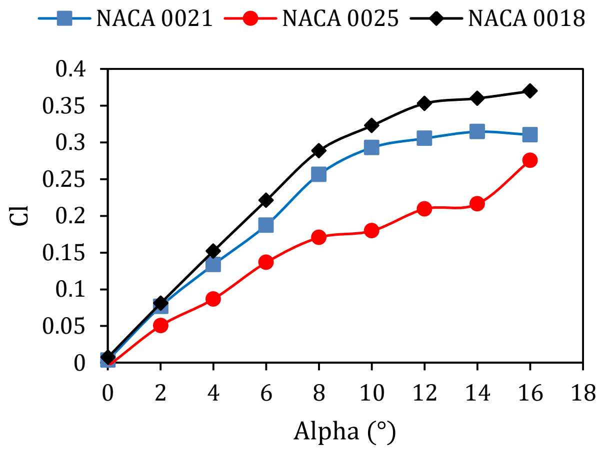

(a)

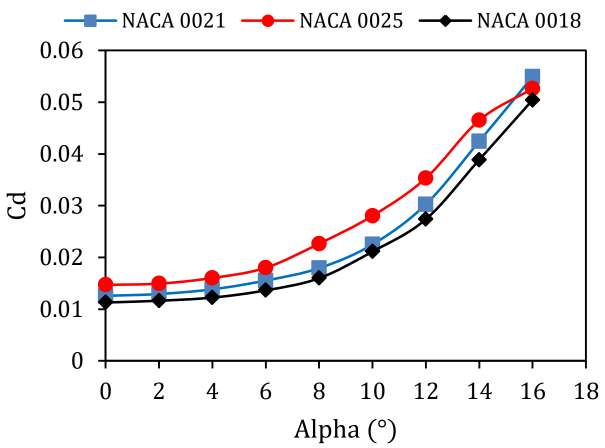

(b)

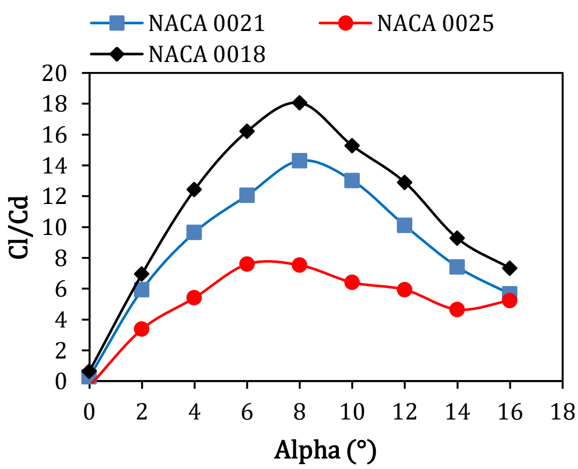

(c)

Figure-4. Lift coefficients (a), drag (b) and polar curve (c) for the preselected airfoils at different angles of attack, obtained in ANSYS-FLUENT.

3.3 Airfoil Selection

The airfoil selected for the VAWT is the NACA 0018, because its lift-drag ratio is superior or close, in a wide range of angles, to those of the other candidates, and also because it has a behavior in its lift coefficient with a linear and increasing trend, without negative changes or drops, which makes it favorable for power generation, as shown in Figure 4. On the other hand, up to angles of attack less than 11° it has a drag coefficient lower than the rest of the airfoils. This selection is also made taking into account the good performance obtained by this airfoil in the CFD simulation.

3.4 Rotor Dimensions

In rotor design, it is always recommended to have high robustness values at low TSR number, therefore, looking for the highest possible power coefficient, the values of 0.5 and 3 are chosen, respectively, which provide a power coefficient (Cp) of 0,42 [17].

Initially, it is established that the turbine will have 3 blades, because studies show that, at this number, the negative torques are reduced, increasing the self-starting capacity [18], and likewise, they provide greater stability [10]. A radius of 1 m is established for the rotor.

From the rotor robustness formula, the optimum chord for the NACA 0018 profile is found, according to equation (3).

$$\sigma = \frac{N \cdot C}{2 \cdot R} \tag{3}$$

Where; N is the number of blades installed, C is the chord of the blades, R is the radius of the rotor.

Likewise, indicating that the power captured by the rotor (Pm), which in this case is 30W, it was possible to determine the swept area of the turbine from equation (4), equivalent to the multiplication of the rotor diameter (D) with the rotor height (h).

$$P_m = 0{,}5 \cdot C_p \cdot \rho \cdot A \cdot V^3 \tag{4}$$

Where; A is the swept area, V is the air velocity and ρ is the air density.

With the above, the dimensions and parameters with which the rotor must comply are determined, which are shown in Table-1. It is necessary to take into account that the TSR indicates the relation between the tangential velocity of the blades and the wind speed, as shown in equation (5)

$$TSR = \frac{\omega \cdot R}{V} \tag{5}$$

Where; ω is the angular velocity of the rotor, R is the radius of the rotor and V is the flow velocity.

ARPN Journal of Engineering and Applied Sciences

www.arpnjournals.com

Table-1. Rotor dimensions and parameters.

Parameters	
Cord length (m)	**0,33**
Number of blades	3
Rotor radius (m)	1
Rotor height (m)	2,16
Rotor solids	0,5
TSR	3
Angular velocity (rad/s)	9

3.5 CFD Analysis of the Rotor

The results presented in Figure-5 indicate that during the 1.5-second simulation study the tangential speed of the blades is approximately 9, 04 m/s, from which if we consider that the tangential speed is equal to the radius (1 m) times the angular speed, we would obtain that the rotor is rotating at 9,04 rad/s, value that was considered since the rotor sizing, so CFD validates the proposed design, obtaining an error percentage of approximately 4%.

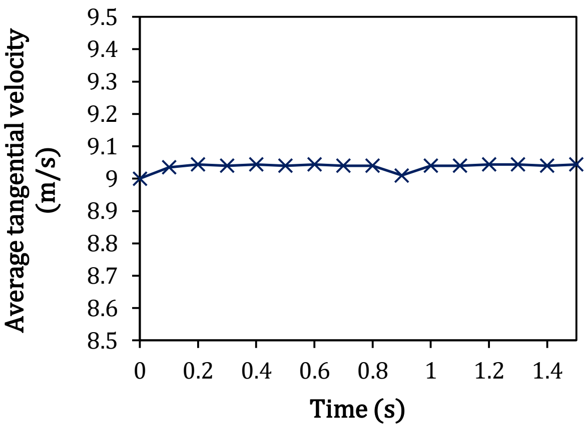

Figure-5. Tangential velocity by rotor average.

Figure-6 shows the velocity contour that develops over the turbine at 1.5 s. It is evident that the highest velocities are generated very close to the rotor blades, while a low-velocity zone is generated inside the rotor.

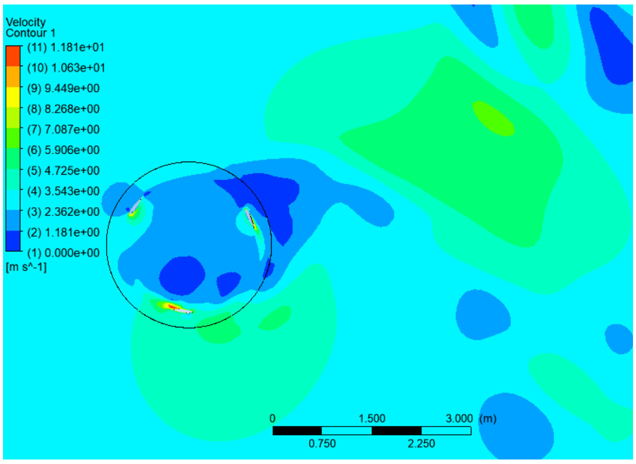

Figure-6. Wind speed contour at 1,5 s

4. CONCLUSIONS

The NACA 0018 profile showed a stable behavior of its lift coefficient at the low wind speed experienced, which demonstrates its potential in the operation of vertical axis wind turbines at low Reynolds numbers and its slight superiority to the NACA 0025 and NACA 0022 profiles.

A vertical axis wind turbine type H with 3 blades, with chord lengths of 0,33 meters, capable of generating a nominal power of 30 W with rotor dimensions of 2 meters in diameter and 2,16 meters in height, at low speeds, working at a TSR equal to 3, is proposed. The results found in the CFD simulation were satisfactory, finding agreement between the angular velocity experienced by the blades in interaction with the wind at a speed of 3 m/s, and the angular velocity obtained theoretically.

REFERENCES

[1] J. Mendoza, J. Rhenals-Julio, A. Avila and E. Durando. 2021. Análise Exergoeconômica da Gasificação de Sabugo de Milho Integrado emum Sistema de Geração de Energia: Estudo de Caso na Colômbia. Rev. virtual Quim. (76): 1-7.

[2] R. E. Hernández, S. A. Méndez, F. R. Ramos and R. A. Munoz. Propuesta de Diseño para el Análisis de Diferentes Perfiles NACA Aplicado a Turbinas Eólicas Horizontales.

[3] S. Li *et al.* 2021. Experimental investigation of solidity and other characteristics on dual vertical axis wind turbines in an urban environment. Energy Convers. Manag. 229: 113689.

[4] J. Bartl, K. F. Sagmo, T. Bracchi and L. Sætran. 2019. Performance of the NREL S826 airfoil at low to moderate Reynolds numbers-A reference experiment for CFD models. Eur. J. Mech. 75: 180-192.

[5] K. S. Patel, S. B. Patel, U. B. Patel and A. P. Ahuja. 2014. CFD Analysis of an Aerofoil. Int. J. Eng. Res. 3(3): 154-158.

[6] A. Dash. 2016. CFD Analysis of Wind Turbine Airfoil at Various Angles of Attack. IOSR J. Mech. Civ. Eng. 13: 18-24.

[7] B. Cheng, J. Du and Y. Yao. 2022. Machine learning methods to assist structure design and optimization of Dual Darrieus Wind Turbines. Energy, 244: 122643, doi: https://doi.org/10.1016/j.energy.2021.122643.

[8] M. F. Almanza Vargas and N. Rodríguez Ribero. 2020. Diseño de un aerogenerador de eje vertical con guía paso a paso para su implementación en una finca de 2000 M2. Fundación Universidad de América.

[9] M. Murshed, M. Y. Arafat and M. A. Razzak. 2019. Analysis of Air Foils and Design of Blades for a Low-Speed 250W Vertical Axis Wind Turbine Suitable for Coastal Areas of Bangladesh. in 2019 1st International Conference on Advances in Science, Engineering and Robotics Technology (ICASERT). pp. 1-6.

[10] A. González-Díaz, L. Geovo-Coronado and Y. González-Doria. 2016. Diseño y modelamiento de un aerogenerador Vawt Darrieus tipo H para la zona costera del departamento de Córdoba. Ingeniare. (20): 33-46.

[11] R. Lanzafame, S. Mauro and M. Messina. 2013. Wind turbine CFD modeling using a correlation-based transitional model. Renew. Energy. 52: 31-39, doi: https://doi.org/10.1016/j.renene.2012.10.007.

[12] F. Balduzzi, A. Bianchini, R. Maleci, G. Ferrara and L. Ferrari; 2016. Critical issues in the CFD simulation of Darrieus wind turbines. Renew. Energy, 85: 419-435, doi: https://doi.org/10.1016/j.renene.2015.06.048.

[13] A. Rezaeiha, H. Montazeri, and B. Blocken. 2019. On the accuracy of turbulence models for CFD simulations of vertical axis wind turbines. Energy. 180: 838-857.

[14] S. Cáceres. 204. Estudio y modelamiento de una turbina eólica de eje vertical de pequeña escala. SANTIAGO DE CHILE.

[15] J. C. Romero Huertas. 2019. Determinación de los valores de arrastre y sustentación de las superficies alares de un dron de ala fija.

[16] C. M. Arenas Burbano and W. R. Quiroga Cortés. 2018. Modelado Y Simulación Aerodinámica De Un Perfil De Microturbina Eólica De Eje Vertical Darrieus Tipo H De Tres Álabes.

[17] Vawt. 2014. Solidity a defining parameter - VAWTVAWT. https://vawt.ro/2014/05/31/soliditate/

[18] N. E. T. Tobón, K. A. H. González, A. F. B. Hernandez, J. S. Del Rio and D. A. H. Zuluaga. 2020. Influencia de la solidez y el número de álabes en una turbina de eje vertical tipo h-darrieus. Rev. Politécnica. 16(32): 9-18.